Available online at www.sciencedirect.com

ScienceDirect

Procedia Engineering 130 (2015) 1273 – 1287

Procedia Engineering

www.elsevier.com/locate/procedia

14th International Conference on Pressure Vessel Technology

Fracture Assessment of Axial Crack in Steel Pipe under Internal Pressure

M. El-Sayed[a], A. El Domiaty[a], A-H.I. Mourad[b,*]

[a]*Mechanical Engineering Department, Faculty of Engineering, Suez Canal University, Ismailia, Egypt*
[b]*Mechanical Engineering Department, Faculty of Engineering, United Arab Emirates University, Arab Emirates*

Abstract

Fracture assessment of axial crack in steel pipe subjected to internal pressure is reviewed. Assessment results were obtained using different methods FC, GS and FAD in order to compare between their results and facilitate their use in any maintenance program. Material type and crack geometry are considered as the main two parameters controlling the failure of the pipe. The constitutive equation of the material is represented by the Ramberg – Osgood model. Six different half crack lengths (40, 60, 80, 100, 120 ,and 140 mm) and four values of the ratio between the crack depth and the pipe thickness are considered (0.2, 0.4, 0.6 and 0.8). The relationship between the fracture parameters (i.e., stress intensity factor K and the J-integral) and the crack length for each assessment method is used. The material properties, plane strain fracture toughness K_{Ic} as well as the critical value of J-integral J_{cr}, are used to determine the critical crack size under specified internal pressure. The assessment method that gives smaller critical crack size is the one which is more conservative than the others. The results obtained by using GS and FAD assessment methods show this type of conservation.

Peer-review under responsibility of the organizing committee of ICPVT-14

Keywords: Fracture Assessment, Axial Surface Crack; Crack Geometry, J-integral, Stress Intensity Factor; Internal Pressure

1. Introduction

Engineering structures such as pipelines often have material defects and geometrical imperfections due to design and manufacturing processes. Under certain loading conditions during service, these defects can grow and gradually

* Corresponding author. Tel.: +971 3 713 5116; fax: +971-3-7134998.
E-mail address: ahmourad@uaeu.ac.ae

Peer-review under responsibility of the organizing committee of ICPVT-14
doi:10.1016/j.proeng.2015.12.297

shorten the residual life or cause a catastrophic failure [1-6]. Using fracture mechanics it is possible to assess the threat of such defects in order to carry out the appropriate maintenance procedure. Presence of defects in the wall of a pipe is generally accepted and detected by nondestructive testing techniques. Controlling rupture risk due to the presence of such defects is the major objective of the maintenance program. Whenever the defect is detected in the pipe, the maintenance team may take one of the following actions: replacing the defected section of the pipe or repairing, and conserving the defect as it is while continuing to use the pipe without any action.

Methods for assessment of damaged pipe under pressure are of great importance and attracted the attention of many researchers [7-13] and the stress intensity factor *K* and *J*-integral formulas available in theses references are listed in table 1. If the pipeline is made of a high-toughness material, the plastic strains become extensive before the crack reaches instability. Hence, some elasto-plastic fracture mechanics parameter, such as the *J*-integral or crack opening displacement *COD/COA* [14-22], or a two-criterion method, should be employed to assess the threat that the crack poses to the pipeline wall. Although cracks of various directions may occur in the pipe wall, we will consider here only longitudinal cracks, because they are subjected to the biggest stress (hoop stress) in the pipe wall. In this study a fracture mechanics approach is used to predict the fracture condition of steel pipes with axial crack. The approach utilizes simple approximate expressions for determining fracture parameters *K* and *J* concerning the axial part-through thickness cracks in a pipe wall. The approach employs these parameters to determine the critical dimensions of a crack on the basis of equality between the *J*-integral and the *J*-based fracture toughness of the pipe steel.

Nomenclature

a	crack depth
c	half crack length
D	outer diameter of the pipe
E	Young's modulus
E`	effective modulus of elasticity
J	crack driving force, *J*-integral
J_{cr}	plane strain fracture toughness
J_e	elastic component of *J*-integral
J_p	plastic component of *J*-integral
K	stress intensity factor
K_{Ic}	plane strain fracture toughness
K_r	non dimensional crack driving force
L_r	non dimensional applied stress
$L_{r,max}$	localized plastic collapse limit
M_T	folias correction factor
n	strain hardening exponent
p	internal pressure
R_o	outer radius
R_i	inner radius
R_m	mean radius
t	pipe wall thickness
φ	angular parameter characterizing crack front position
υ	poisson´s ratio
σ_o, σ_y	yield stress
σ_u	ultimate stress
σ_φ	hoop stress
FAD	failure assessment diagram
COD	crack opening displacement
COA	crack opening angle

Table 1. Stress intensity factor and *J*-integral for axial crack in pipe.

Reference	Stress intensity factor (K)	J–integral
Ľubomír Gajdoš and Martin Šperl [7].	$K_I = \left[M_F + \left(E_{(k)}\sqrt{c/a} - M_F \right) \left(\frac{a}{t} \right)^s \right] \frac{\sigma_\varphi \sqrt{\pi a}}{E_{(k)}} M_{TM}$	The FC method $J = \frac{K^2}{E} \left[A + \frac{0.5\left(\sigma/\sigma_0\right)^2}{A} \right]$ The GS method $J = \frac{K^2}{E} \left[1 + \frac{2\alpha n}{(n+1)} \left(\frac{\sigma}{\sigma_0} \right)^{n-1} \right]$
I.Skozirt, Z.Tonkovic, "Numerical [8].		$J_{ep} = J_{el} + J_{pl}$ $J_{el} = \left(\frac{pR_m}{t} \right)^2 \pi a.F^2 \left(\frac{R_m}{t}, \frac{a}{t}, \frac{c}{a}, \varphi \right) \Big/ E$ $J_{pl} = \alpha \frac{\sigma_y^2}{E} (t-a) h_1 \left(\frac{R_m}{t}, \frac{a}{t}, \frac{c}{a}, \varphi \right) \left(\frac{p}{p_L} \right)^{n+1}$
Rishi Kumar Sharma, S. K. Shrivastava, P. M. [9].		$J(\varphi) = \alpha \frac{\sigma_0^2}{E} (t-a) h_1 \left(\frac{R}{t}, \frac{a}{t}, \rho, \varphi, n \right) \left(\frac{p}{p_L} \right)^{n+1}$
Z. Tonković, et al [10].	The linear – elastic $K = \left(\frac{pR_m}{t} \right) \sqrt{\pi a} F \left(\frac{R_m}{t}, \frac{a}{t}, \rho, \varphi \right)$	$J = J_e + J_p$ $J_p = \alpha \frac{\sigma_y^2}{E} (t-a) h_1 \left(\frac{a}{t}, c \right) \left(\frac{p}{p_L} \right)^{n+1}$
Ž. Šarkoćević, et. al. [11].	$k_I = \sqrt{\frac{\pi a}{Q}} \frac{pR_i^2}{R_o^2 - R_i^2} 2G_0 + 2\frac{a}{R_i} G_1 + 3\frac{a}{R_i}^2 G_2 + 4\frac{a}{R_i}^3 G_3$	

In failure assessment diagram (FAD) method, the limit load of a cracked pipe is used to define a parameter L_r that measures the proximity to plastic collapse. Moreover, when the structural assessment integrity is done using the R6 method, the reference stress is defined by the limit load. Here, the limit load is usually estimated on damage in high strength steels. A large number of existing solutions to pressure limit of the damaged pipes is developed analytically and empirically on the basis of the data obtained by testing [8-10].

The crack tip constraint is taken into account by the so-called plastic constraint factor *C*, by which the uniaxial yield stress in the *J*-integral equation is multiplied [7]. There are a lot of studies have been reported in the area dealing with the determination of the *J*-integral and plastic limit load for metal pipes with external axial semi-elliptical surface cracks [8]. In general, the *J*-integral is expected to be a function of the quantities which are based on pipe and crack dimensions, and material parameters [9]. The results for the stress intensity factors and *J*-integral are generated and expressed as the GE/EPRI influence functions to allow comparisons with the values available in literature [10]. In addition to the experimental research, based on the obtained values for K_r and L_r using the fracture analysis diagram (FAD) is carried out an assessment of the integrity of pipes with an axial surface crack on the outer surface [11].

The objective of the present work is to carry out an evaluation and comparison between the assessment methods based on their applicability to detect the effect of material type and crack geometry on the critical crack length or the maximum operating pressure.

2. Theoretical analysis of axial cracks in pipes

2.1. Stress intensity factor for a longitudinal through crack in the pipe wall

An expression for the stress intensity factor for a long cylindrical pipe with a longitudinal through crack under internal pressure was reported by Folias [25] and by Erdogan and Kibler [26]. They managed to show that the problem was analogous to that of a wide plane plate with a through crack. The only adjustment needed for transition to a pipe was to introduce a correction factor to multiply the solution for the plane plate. This factor, frequently referred to as the Folias correction factor and designated by symbol M_T. This factor is only a function of the ratio $\lambda = c/\sqrt{R_m t}$, where c is the crack half-length, R_m is the pipe mean radius, and t is the pipe wall thickness. Thus it depends only on the geometrical parameters of the crack and the pipe Fig. 1.

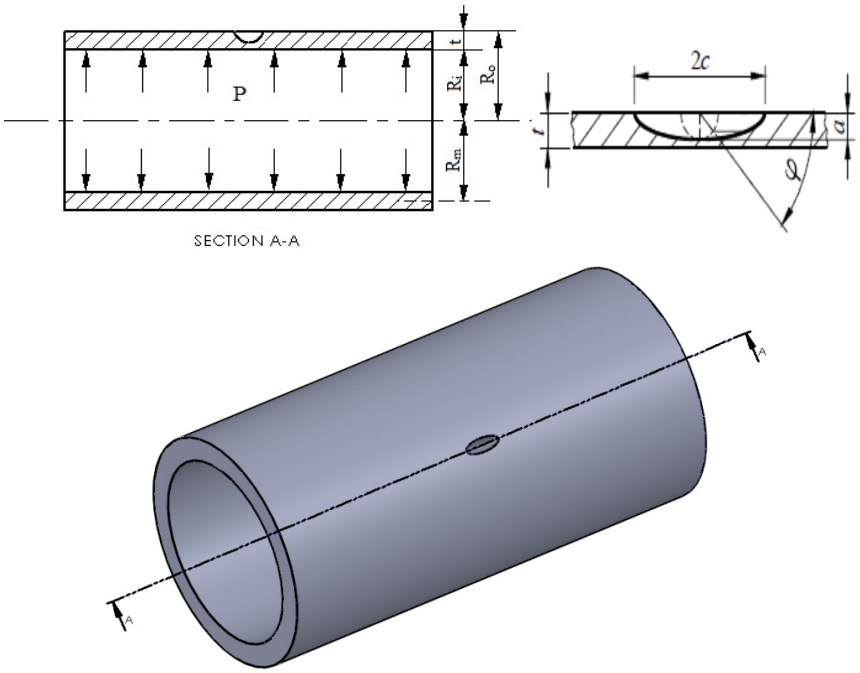

Fig. 1. Geometry and dimensions of a pipe subjected to internal pressure with an external axial semi-elliptical surface crack.

Several relations have been reported for determining the Folias correction factor [27]. The following are the most frequently used at the present time:

The Folias relation [27]:

$$M_T = \sqrt{1 + 1.255\lambda^2 - 0.0135\lambda^4} \tag{1}$$

The Erdogan et al. relation [28]:

$$M_T = 0.6 + 0.5\lambda + 0.4\exp(-1.25\lambda) \qquad \text{for} \quad \omega < 5 \tag{2}$$

$$M_T = 1.761(\lambda - 1.9) \qquad \text{for} \quad \omega \geq 5$$

where $\omega = \sqrt[4]{12(1-\upsilon^2)}\lambda$

with υ denoting Poisson´s ratio

The following relation is the simplest:

$$M_T = \sqrt{1+1.6\lambda^2} \tag{3}$$

However, its validity is limited by the value λ<1. Since the c is the half-length of a longitudinal through crack in the pipe, then the stress intensity factor of such a crack simply reads

$$K_I = M_T \sigma_\varphi \sqrt{\pi c} \tag{4}$$

where

$\sigma_\varphi = {p.D}/{2t}$ is the hoop stress (D and t denoting pipe diameter and wall thickness, respectively), and M_T is the Folias correction factor

2.2. Stress intensity factor for a longitudinal part-through crack

Various methods are used for analyzing the problem of longitudinal semi-elliptical surface cracks in the wall of cylindrical shells (Fig. 2). Finite element method and the method of boundary integral equations, or various alternative methods (e.g. the weight function method) are used to estimate the stress intensity factor . The first solutions for semi-elliptical surface cracks in a plate subjected to uniaxial tension or steady bending were derived from solutions for an elliptical plane crack in an infinite 3D body. In order to account for the finite thickness of a body and the plastic zone at the crack tip, correction factors were introduced for the "front" surface and the "rear" surface of the body and for the plastic region at the crack tip [29]. However, solutions by different authors often showed rather considerable disagreement. Scott and Thorpe [30] therefore tested the accuracy of the solutions presented by various authors by measuring changes in the shape of a crack throughout its fatigue growth. They concluded that the best engineering estimation of the stress intensity factor for a part through crack in a plate was provided by Newman's solution [31]. An adjusted form of this solution for a thin-walled shell is given by:

$$K_I = \left[M_F + \left(E_{(k)}\sqrt{c/a} - M_F \right) \left(\frac{a}{t} \right)^s \right] \frac{\sigma_\varphi \sqrt{\pi a}}{E_{(k)}} M_{TM} \tag{5}$$

where

M_F is the function depending on the crack geometry (on the ratio a/c)

$$M_F = \sqrt{\frac{c}{a}} \left[1 + 0.03 \left(\frac{c}{a} \right) \right] \qquad \text{for } \frac{a}{c} > 1$$

and, $M_F = 1.13 - 0.1\left(\frac{a}{c} \right)$ for $0.02 \le \frac{a}{c} \le 1$

$E_{(k)} = \int_0^{n/2} \sqrt{1-k^2 \sin^2\theta}\, d\theta$ is an elliptical integral of the second kind, k being $\sqrt{1-\left(\frac{a}{c} \right)^2}$

$$E_{(k)} = 1 + 1.464\left(\frac{a}{c}\right)^{1.65}$$

s is a function depending on the crack geometry, the ratio *a/c* , and the relative crack depth, the ratio *a/t*.

$$s = 2 + 8\left(\frac{a}{c}\right)^{3} \text{ for } 0.02 \le \frac{a}{c} \le 1$$

$M_{TM} = \dfrac{\left(1 - \dfrac{a/t}{M_T}\right)}{\left(1 - a/t\right)}$ is the correction factor for the curvature of a cylindrical shell and for an increase in stress owing to radial strains in the vicinity of the crack root , as is shown in Fig.2.

In the last relationship, M_T is the Folias correction factor, determined by any of the relations (1) – (3). The functions M_F and *s* differ in form for the lowest point of the crack tip (point A in Fig. 2) and for the crack mouth on the surface of the cylindrical shell (point B in Fig. 2).

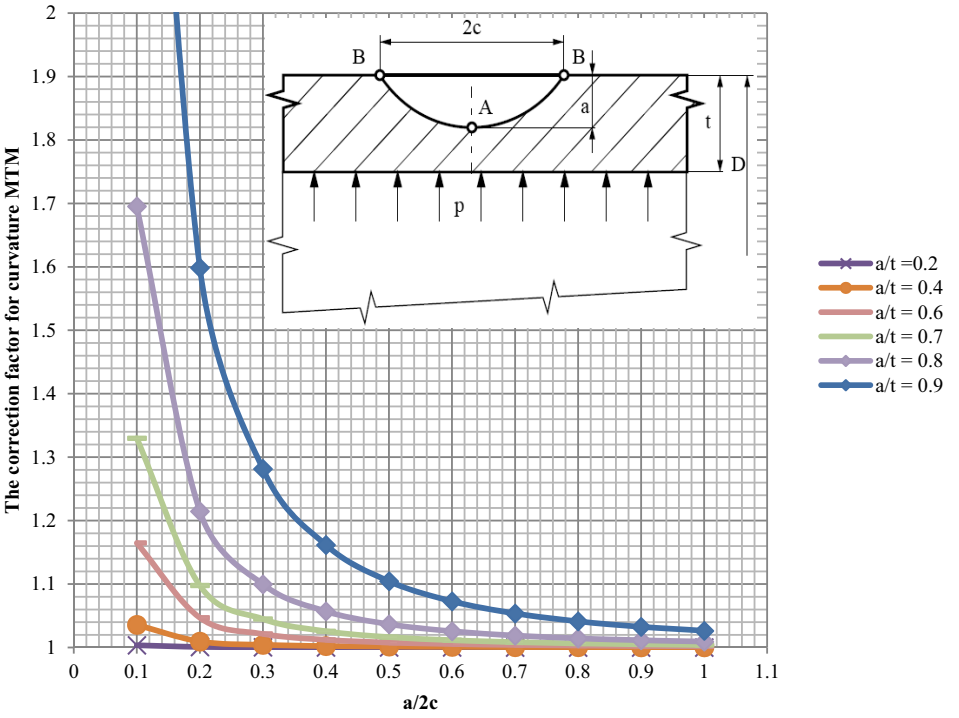

Fig. 2. The geometrical parameter M_{TM} as function of the crack geometry.

2.3. Engineering Methods for Determining the J-integral

2.4. The Folin–Ciocalteu (FC) method

This method was proposed in Addendum A16 of the French nuclear code [32]. It stems from the second option for describing the transition state between ideally elastic and fully plastic behavior of a material. as suggested in the R6 method [33]. Considering the Ramberg-Osgood form of the stress-strain dependence Eq. (6) we can arrive at Eq. (7):

$$\frac{\varepsilon}{\varepsilon_o} = \frac{\sigma}{\sigma_o} + \alpha\left(\frac{\sigma}{\sigma_o}\right)^n \tag{6}$$

$$J = \frac{K^2}{E`}\left[A + \frac{0.5\left(\sigma/\sigma_0\right)^2}{A}\right] \tag{7}$$

where

σ_0 is usually taken as the yield stress and $\varepsilon_0 = \sigma_0 / E$

α, n are material constants

$E` = \frac{E}{1-\upsilon^2}$ for the plane stress, and E` = E for the plane strain

υ is Poisson´s ratio

$$A = 1 + \alpha\left(\frac{\sigma}{\sigma_0}\right)^n \tag{8}$$

As a pipeline is a body of finite dimensions, stress σ in Eqs. (7) and (8) is a nominal stress – i.e. a stress acting in the plane where the crack occurs. Referring to the R6 method [33], this stress for a pipe containing a longitudinal part-through thickness crack may be written as:

$$\sigma = \frac{\sigma_\varphi}{1 - \frac{\pi ac}{2t\left(t+2c\right)}} \tag{9}$$

In eq. (9), $\sigma_\varphi = \frac{p.D}{2t}$ is the hoop stress,

2.5. The Gauss–Seidel (GS) method

The GS method was derived by Gajdoš and Srnec [34] on the basis of the limit transition of the *J*-integral, formally expressed for a semi-circular notch, to a crack, with the variation of the strain energy density along the notch circumference being approximated by the third power of the cosine function of the polar angle. If the stress-

strain dependence is further expressed by the Ramberg-Osgood relation (6), with $\varepsilon_0 = \sigma_0 / E$, (α, n – material constants), we can arrive at Eq. (10)

$$J = \frac{K^2}{E}\left[1 + \frac{2\alpha n}{(n+1)}\left(\frac{\sigma}{\sigma_0}\right)^{n-1}\right] \tag{10}$$

3. Consideration of the constraint

As mentioned above, the situation existing at the crack tip in conditions of small-scale yielding can be characterized by a single fracture parameter (e.g. *K*, *J* or *COD*) [14-22]. This parameter can be used as a fracture criterion, independent of geometry. However, single-parameter fracture mechanics fails in cases of developed plasticity, where fracture toughness is a function not only of the material, but also of the dimensions and the geometry of the specimen. It is well known from the theory of fracture mechanics that for small-scale yielding the maximum stress existing at the crack tip in a non-hardening material is about $3\sigma_o$, where σ_o is the yield stress. Single-parameter fracture mechanics apparently does not apply to non-hardening materials under fully plastic conditions, because the stress and strain fields in the vicinity of the crack tip are affected by configurations of both the body and the crack. The situation is more favorable in hardening materials, where single parameter fracture mechanics may approximately apply also for the developed plasticity, provided that the body maintains a high level of stress triaxiality.

3.1. Plastic constraint factor on yielding

A simple procedure based on the use of the plastic constraint factor on yielding, *C*, can be applied to determine the fracture conditions in a thin-walled pressure pipeline. The factor is given by the ratio of the stress needed to obtain plastic macrostrains under constraint conditions to the yield stress at a homogeneous uniaxial state of stress [35]. The *C* factor can be expressed by Eq. (11).

$$C = \frac{\sigma_1}{\sigma_{HMH}} \tag{11}$$

where σ_{HMH} the Huber-Mises-Hencky stress, is put equal to the yield stress.

Let us now consider the state of stress at the crack tip in a thick-walled body, where the stress perpendicular to the crack plane, σ_1,and the stress in the direction of the crack, σ_2, are equal, and the stress in the direction of the thickness of the body, σ_3, is governed by the expression $\sigma_3 = \upsilon(\sigma_1 + \sigma_2)$. Then, based on the HMH criterion and assumed elastic conditions ($\upsilon \cong 0.33$), the plastic constraint factor $C \approx 3$. If the stress in the thickness direction, σ_3, falls between $2\upsilon\sigma_1$ and zero (thin-walled body), the value of the plastic constraint factor will range between C =1 and *C* = 3. This data can be used to assess the fracture conditions in gas pipelines with surface part-through cracks, employing a *C*-factor which has to be experimentally determined. After the *C* factor has been determined, the value of $C\sigma_o$ would be used instead of the yield stress σ_o in relations for calculating the *J*-integral. The *C* factor was experimentally investigated at the Institute of Theoretical and Applied Mechanics of the Academy of Sciences of the Czech Republic in the framework of a broader research project on the reliability and operational safety of high pressure gas pipelines.

Fracture conditions were investigated on five pipe bodies, made of steels X52, X65 and X70, with cycling induced cracks. Data on the pipe and surface crack geometries, internal pressure and material properties are given in Table 2. Two methods, namely FC and GS, can be used to obtain the values of *J*-integral as a function of the initial crack depth by using Eqs. (7) and (10). Therefore, the methods can be used to determine the critical crack depth of cracked pipes.

Table 2. Summary of pipe data used in the assessment of the fracture behaviour

Material	X 52	X 65	X 65	X70	X70
D (mm)	820	820	820	1018	1018
t (mm)	10.2	10.7	10.6	11.7	11.7
c (mm)	50	100	100	127	115
a (mm)	7	7.7	7	6.7	7.1
a/t	0.686	0.720	0.660	0.573	0.607
a/c	0.14	0.077	0.07	0.053	0.062
p (MPa)	9.36	9.71	9.86	9.86	9.55
σ_0 (MPa)	395	496	496	536	536
α	5.87	5.34	5.34	5.92	5.92
n	8.24	8.45	8.45	9.62	9.62
C	2.2	2.4	2.3	2.07	2
J_{cr} (N/mm)	415	432	432	439	439

Figure 3a shows the values of *J*-integral obtained at different crack depth using the both methods (FC and GS) for a pipe made of X70. The pipe dimensions and material properties are shown in the figure. The material toughness is given as J_{cr} = 439 N/mm [1]. It can be seen that the two methods predict almost the same values of *J*-integral up to crack depth of 7.1 mm. However, the difference between the estimated *J*-integral using the two methods increases as the crack depth increases. By drawing a horizontal line at $J=J_{cr}$, the critical crack depth was found to be 7.18 mm using the FC method and to be 7.09 mm using the GS method. These results indicate that either of the method can be used to predict the critical crack depth accurately with only difference of 1.3%.

The variation of the *J*-integral with the crack depth for X52 steel is demonstrated in Fig. 3b the trend of variation is exponential and similar to that of X70. The intersection of the horizontal line $J = J_{cr}$ = 415 N/mm with the two (J – a) curves according to the FC and GS methods gives the value of critical crack depth a_{cr} = 7.12 mm according to FC method, and a_{cr} = 6.89 mm according to GS method. There is a slight difference of 3.3% between the two methods.

Figure 4a and 4b demonstrates the variation of *J*-integral with crack depth to pipe thickness ratio $(a/t)_{cr}$ for different half crack length *c* using the FC and GS Methods, respectively.

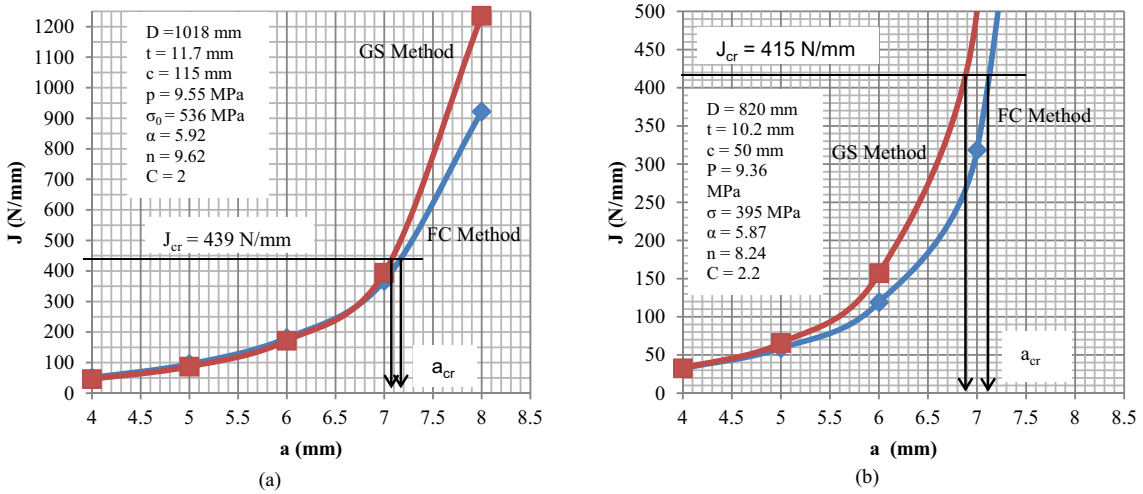

Fig. 3. Variation of *J*-integral with crack depth *a* using FC and GS methods for (a) X70 steel; (b) X52 steel.

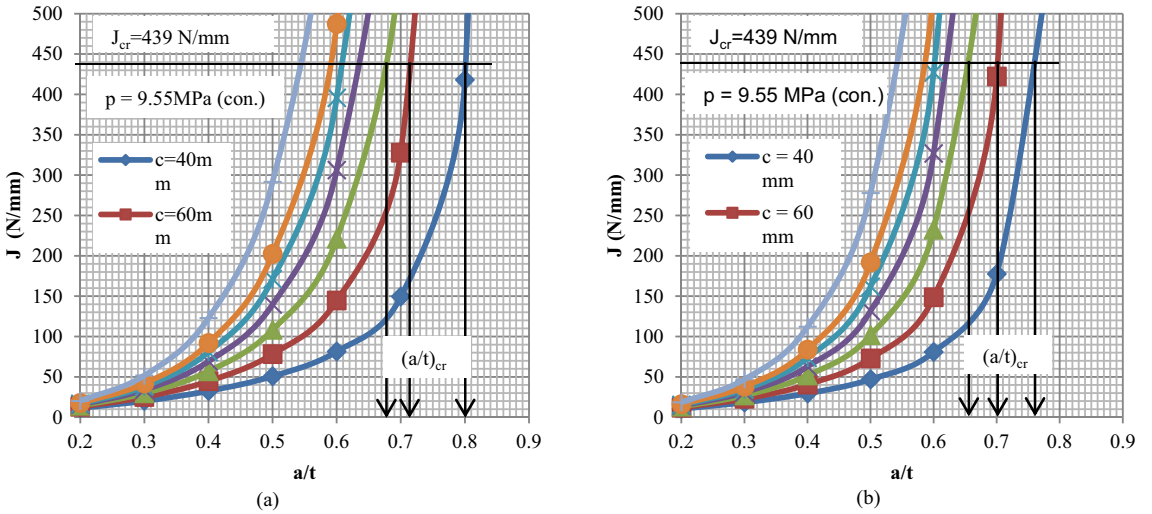

Fig. 4. Prediction of the critical ratio of the crack depth to pipe thickness (a/t)cr for different half crack length c (a) FC Method; (b) GS Method.

As obvious from Fig. 4 for material X70 the value of failure relative crack depth $(a/t)_{cr}$ can be obtained by the intersection of the straight line $J = J_{cr} = 439$ N/mm with (J– a/t) curves for different half crack length c and constant pressure of 9.55 MPa. For a crack length $c = 40$ mm, $(a/t)_{cr} = 0.8$ and 0.76 using FC and GS methods, respectively. This shows that, GS method is more conservative.

As the crack length c increases, the relative critical crack depth $(a/t)_{cr}$ decreases. Therefore, the fracture condition depends on the geometry of the crack (c, a, a/t).

Figure 5a and 5b demonstrates the variation of the relative critical crack depth $(a/t)_{cr}$ with the crack length c using FC and GS methods, respectively, for steel X70 and steel X52 at constant pressure. For each crack length there is a corresponding critical value of a/t ratio at a certain pressure. The area under the curve is the safe area while failure will take place for values above the curves. The results reveal that the GS method is a more conservative in predicting the parameters.

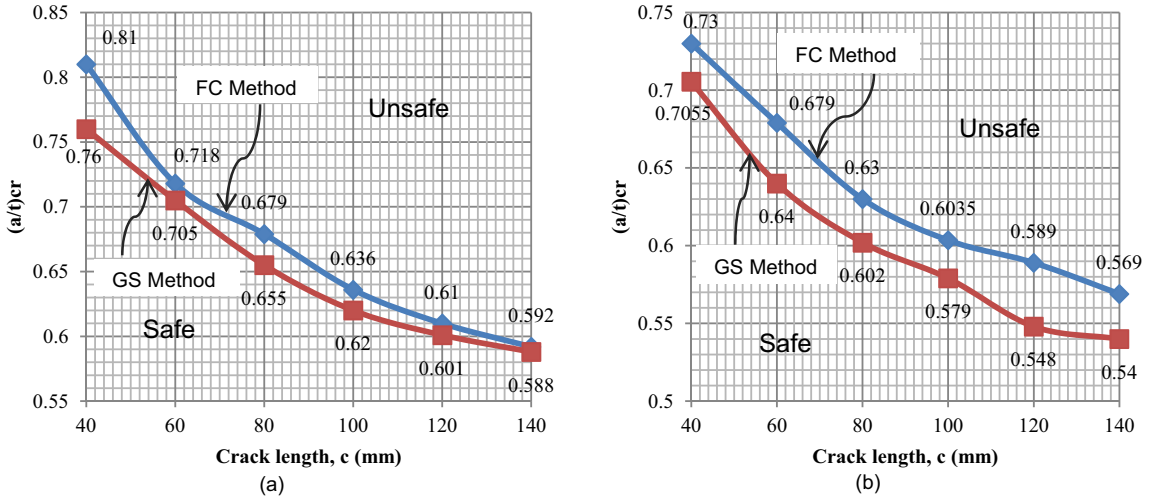

Fig. 5. Variation of the critical ratio of the crack depth to pipe thickness (a/t)cr with crack length c (a) X70 and p= 9.55 MPa; (b) X52 and p= 9.36 MPa.

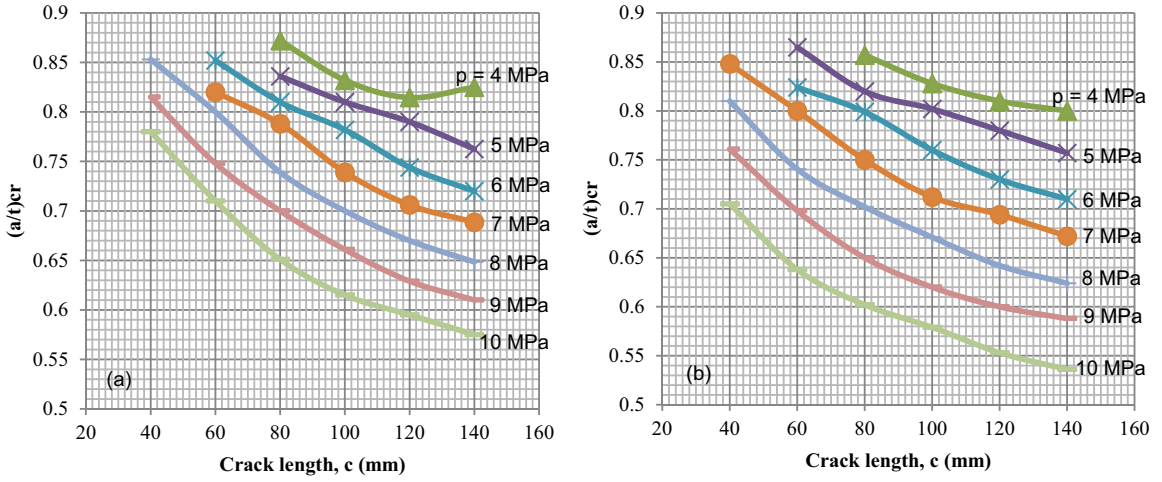

Fig. 6. Variation of the critical ratio of the crack depth to pipe thickness (a/t)cr with Crack length c using FC Method (a) X70 steel; (b) X52 steel.

Figure 6 shows variation of the failure relative crack depth to thickness $(a/t)_{cr}$ ratio with crack length c by using FC method for X70 and X52 under different pressures. As the pressure increases the crack depth decreases and the curve becomes more steeper for higher pressure.

For material X52, Fig. 7 presents the variation of J-integral with the a/t ratio. The critical a/t ratios are corresponding to J_{cr} for different crack length c. When the crack length c= 40 mm, $(a/t)_{cr}$ = 0.73 using FC method and $(a/t)_{cr}$ = 0.706 using GS method which shows that the GS method is more conservative than FC method.

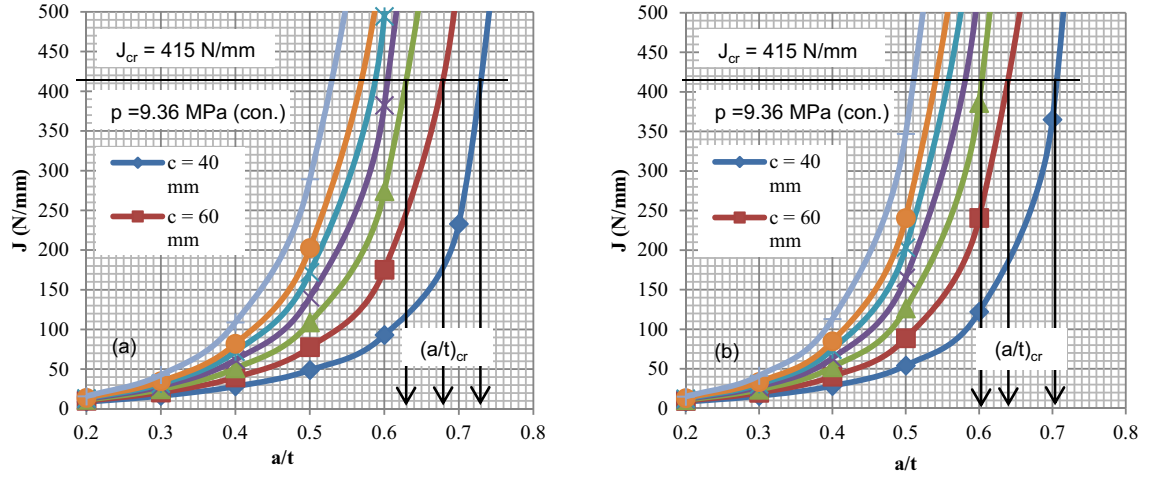

Fig. 7. Prediction of the critical ratio of the crack depth to pipe thickness (a/t)cr for different half crack length c (a) FC Method; (b) GS Method.

4. R6 analysis

The R6 methodology for assessing the integrity of cracked structures was developed and validated by the UK Central Electricity Generating Board (CEGB) [16]. The assessment procedure consists of interpolating between the

linear elastic fracture mechanics criterion for failure and the fully plastic limit-load solution using a failure assessment diagram (FAD). As such, the R6 method is basically a design or failure avoidance procedure with an inherent safety margin already included in the analysis. Crack initiation and maximum-load predictions using this scheme are therefore expected to underestimate the actual or experimentally measured loads.

4.1. Failure assessment diagram (FAD)

R6 introduced the concept of the failure assessment diagram (FAD). To construct this diagram, it is necessary to calculate two parameters, namely, non dimensional crack driving force K_r and non dimensional applied stress L_r. As shown in Fig. 8, the vertical axis of the FAD represents the ratio of applied stress intensity factor to the fracture toughness (K_{Ic}), (i,e. K_r). K_{Ic} is determined from the standard fracture toughness testing, while the horizontal axis is for L_r which represents the ratio of the applied load to the load required to cause plastic collapse of the flawed section. These two parameters are calculated by using the following expressions [11]:

$$K_r = \frac{K_{app}}{K_{Ic}} = \sqrt{\frac{J_{app}}{J_{Ic}}} \tag{12}$$

$$L_r = \frac{\sigma_{app}}{\sigma_f} \tag{13}$$

where

$$\sigma_{app} = \sigma_{hoop} = \frac{P.R_m}{t}$$

$$\sigma_f = \frac{\sigma_y + \sigma_u}{2}$$

σ_y = yield stress and σ_u = ultimate stress

The relationship between K_r and L_r define the boundary line of the failure assessment diagram (FAD). The critical assessment points leading to fracture yield an assessment interpolation curve between two specific or reference limit states. These are brittle fracture state [K_r =1 and L_r = 0] and plastic collapse state [K_r = 0 and L_r =1]. The assessment point of a component can be highlighted by a point of coordinates K_r and L_r. If this point is inside the boundary line of the diagram which is limited by the interpolation curve, the structure is safe. If not, failure occurs and the assessment point is situated outside of the interpolation curve (Fig. 8).

The interpolation curve in terms of non dimensional load is given by the formula [12, 13]:

$$f(L_r) = \frac{1}{\sqrt{\left[1 + \frac{L_r^{\,2}}{2}\right]}} . \left[0.3 + 0.7 \exp\left(-0.65 L_r^{\,6}\right)\right] \quad 0 \le L_r \le L_{r,\max} \tag{14}$$

and the Cut-off ratio is defined using the following equation [7]:

$$L_{r,\max} = 1 + \left[\frac{150}{\sigma_y}\right]^{2.5} \tag{15}$$

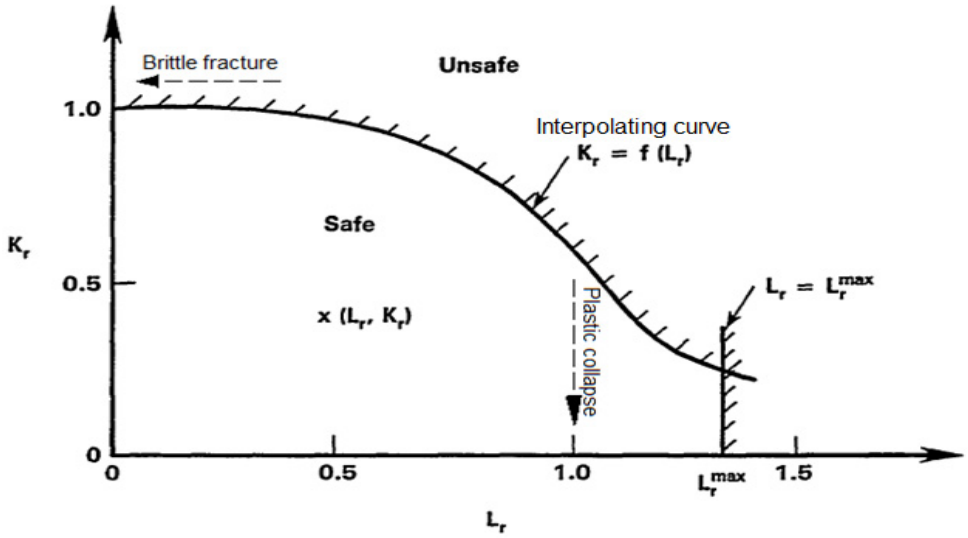

Fig. 8. The failure assessment diagram [16].

For example, Failure Assessment Diagram (FAD) will be applied for pipe with axial surface crack made of X70 steel. Table 3 presents the values of the parameters K_r, and L_r for a=7.1 mm, c=115 mm and t=11.7 mm and different pressure value (0-10 MPa). The Fracture Assessment Diagram (FAD) is plotted in Fig. 9, the failure assessment line is plotted using Eq. (14). The two loading lines have been plotted using Eqs. (12) and (13) knowing J_{app} Eqs. (7) and (10) and applied stress σ_{app}. Calculating J_{app} necessitate the calculation of K_I and σ_{app} which are function of the applied pressure.

A defect in the pipe is acceptable if the calculated values are located inside the failure assessment line. Those outside are unsafe and failure occurs.

Table 3. Values of the parameters of K_r and L_r for a=7.1 mm, c=115 mm, t=11.7 mm.

P (MPa)	$\sigma_{app} = \sigma_\varphi$ (MPa)	k_I (Eq. 5) (MPa$\sqrt{m}$)	J(FC) (N/mm) (Eq.7)	K_r (FC) (Eqs. 12, 7)	J(GS) (N/mm)	K_r (GS) (Eqs. 12, 10)	L_r (Eq. 13)	$K_r = f(L_r)$ (Eq. 14)
0	0	0	0	0	0	0	0	1
1	43.50427	782.5485	3.070354	0.08363	3.061911	0.083515	0.082473	0.999048
2	87.00855	1565.097	12.38274	0.167948	12.24765	0.16703	0.164945	0.996182
3	130.5128	2347.645	28.24119	0.253635	27.5579	0.250548	0.247418	0.991326
4	174.0171	3130.194	51.15443	0.341357	49.00558	0.334111	0.32989	0.984187
5	217.5214	3912.742	81.85551	0.431809	76.70829	0.418012	0.412363	0.974014
6	261.0256	4695.291	121.418	0.525907	111.3417	0.503613	0.494835	0.959299
7	304.5299	5477.839	171.7282	0.625444	155.7541	0.595645	0.577308	0.937473
8	348.0342	6260.388	236.9776	0.734719	219.5838	0.707242	0.65978	0.90474
9	391.5385	7042.936	327.7984	0.864114	330.5327	0.867711	0.742253	0.85633
10	435.0427	7825.485	472.8447	1.037832	558.8258	1.128252	0.824726	0.787623

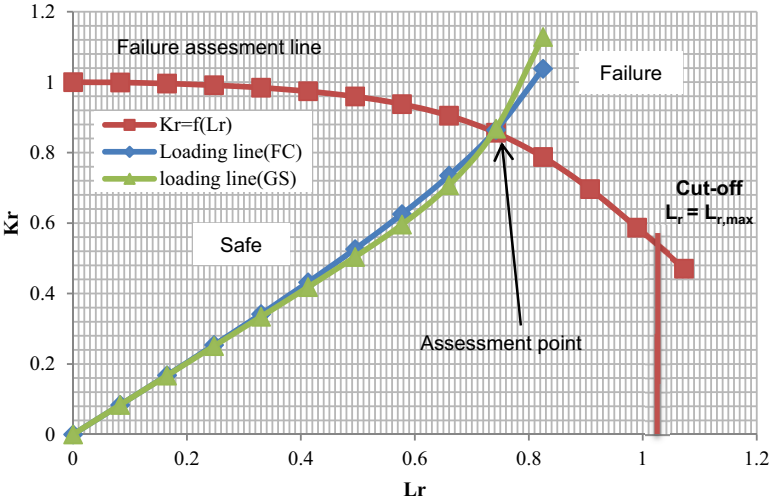

Fig. 9. Fracture analysis diagram (FAD) for pipe with an axial surface crack at various pressure.

5. Conclusion

Three different engineering methods FC, GS and FAD have been worked out for assessing the geometrical parameters of critical axial crack-like defects in a pipeline wall under internal pressure. The methods make use of simple expressions for determining fracture parameters *K* and *J*. The results obtained demonstrate the GS method gives smaller values of the critical crack length under different operating internal pressure. This means that the GS method is more conservative for using it in a maintenance program. Using these assessment methods, the critical pressure in a pipeline can also be determined for a given crack geometry. Much more conservative values for the critical crack geometry under specific operating pressure or the burst pressure for specific crack geometry can be obtained by applying FAD analysis.

Reference

[1] A-H. I. Mourad, J. Altarawneh, A. El Domiaty and Y. J. Chao, 2012, "Fracture Toughness Determined From Full-Scale Pipe", Proc. ASME. 55706; Volume 6A: Materials and Fabrication, PVP Conference, pp. 125-130, Toronto, Ontario, Canada, July 15–19, 2012.

[2] A.-H. I. Mourad; J. Altarawneh; A. El Domiaty, 2013, "Fracture Assessment of X65 Steel Pipe With Through-Wall Crack Under Pure Bending", Proc. ASME. 55706; Volume 6A: Materials and Fabrication, Paris, France, July 14–18, 2013.

[3] A-H.I Mourad, J. altarawneh, A. E. Domiaty, Y. J. Chao, and F. Haggag, 2014, "Fracture Toughness Measurements from Circumferentially-Notched Pipes Tests", special issue on Fracture Toughness, Materials Performance and Characterization, Vol. 3, No. 3, pp 305-321.

[4] A-H.I. Mourad, Aly El-Domiaty, Y J Chao, 2012, Fracture toughness prediction of low alloy steel as a function of specimen notch root radius and size constraints, Engineering Fracture Mechanics, Vol. 103, pp.79–93.

[5] Abdel-Hamid I. Mourad, Aly El-Domiaty, 2011, "Notch Radius and Specimen Size Effects on Fracture Toughness of Low Alloy Steel", Procedia Engineering, Vol.10, pp. 1348-1353.

[6] A-H. I. Mourad, Aladdin Abu-Assi and Fahmy M. Haggag, Yuh J. Chao, 2014, "Novel Technique for Normalizing Load-Displacement Curves in Fracture Testing, Materials Performance and Characterization", special issue on Fracture Toughness, Vol. 3, No. 3, pp 1-20.

[7] Ľubomír Gajdoš and Martin Šperl , 2011 "Application of a Fracture-Mechanics Approach to Gas Pipelines", world Academy of science , Engineering and technology, vol :49, 2011-01-25, pp. 385-392.

[8] I.Skozirt, Z.Tonkovic, 2009, " Numerical Modelling of Creep Fracture Behavior of Medium Density polyethylene (MDPE)", Proceedings of the 12th International Conference on Fracture, M. Elboujdaini (ed.), Ottawa, Canada, 12-17 July 2009, CD-ROM edition, pp. 1-10.

[9] Rishi Kumar Sharma, S.K.Shrivastava, P.M.Dixit and Sumit Basu, 2006, " On the problem of an axial semi-elliptical crack in a hollow ductile cylinder", International Journal of fracture(2006) 140:269-275, pp.269-275.

[10] Z. Tonković, I. Skozrit and J. Sorić, 2005, " A Contribution to Assessment of Steam Generator Tubes Integrity", Proceedings of the 11th International Conference on Fracture, Carpinteri, A. (ed.), Turin, Italy, 20-25 March 2005, CD-ROM edition, pp. 1-6 .
[11] Ž. Šarkoćević, M. Arsić, A. Sedmak, B. Medjo, M. Mišić, 2014, "Assessment of integrity of the welded pipes" , Annals of the university of Oradea ,Issue#2, august 2014, pp. 1-6.
[12] F. W. Brust, P. Scott, S. Rahman, N. Ghadiali, T. KffinsM, B. Francini, 1995, "Assessment of Short Through-Wall Circumferential Cracks in Pipes", Central Research Institute of Electric Power Industry, April 1995, pp. ch.4. 97-101.
[13] T. Boukharouba , 2009," Defect Assessment on Pipe Transporting a Mixture of Natural Gas and Hydrogen", Springer Science , 2009, pp. 19-32.
[14] S. K. Maiti, K. Kishore, and A. -H. I. Mourad, 2008, "Bilinear CTOD/CTOA scheme for characterisation of large range mode I and mixed mode stable crack growth through AISI 4340 steel Nuclear Engineering and Design, Volume 238, issue 12, pp. 3175–3185.
[15] S. K. Maiti, S. Namdeo and A.-H.I. Mourad, 2008, "A scheme for finite element analysis of mode I and mixed mode stable crack growth and a case study with AISI 4340 steel" Nuclear Engineering and Design, Elsevier, Volume 238, Issue 4, pp. 787-800.
[16] A. -H. I. Mourad, M. G. Alghafri, O. A. Abu Zeid and S. K. Maiti, 2005, "Experimental investigation on ductile stable crack growth emanating from wire-cut notch in AISI 4340 steel", Nuclear Engineering and Design, Volume 235, Issue 6, pp. 637-647.
[17] A.-H.- I. Mourad and S .K Maiti, 1996, "Mode II stable crack growth", Fatigue and Fracture of Engineering Materials and Structures, The International Journal, The official Journal of ESIS the ESIS, Vol. 19, pp. 75-84.
[18] A.-H. I. Mourad and S .K Maiti, 1995, "Mode I and mixed mode stable crack extensions through stiffened TPB specimens", Fatigue and Fracture of Engineering Materials and Structures, The International Journal, The official Journal of ESIS Vol. 18, pp. 648-652.
[19] S. K. Maiti, and A.-H. I. Mourad,1995, "Criterion for mixed mode stable crack growth-part I. Three point bend geometry", Engineering Fracture Mechanics, Published by Elsevier Science Ltd, Vol. 52, pp. 321-347.
[20] S. K. Maiti and A.-H. I. Mourad,1995, "Criterion for mixed mode stable crack growth-part II. Compact tension geometry with and without stiffener", Engineering Fracture Mechanics, Vol. 52, pp. 349-378.
[21] A.-H. I. Mourad and S .K. Maiti, 1995, Influence of state of stress on mixed mode stable crack growth through D16AT aluminium alloy, International Journal of Fracture, Vol. 72, pp. 241-258.
[22] A.-H. I. Mourad and S .K. Maiti, 1995, "Influence of state of stress on mode I and mixed mode stable crack growth through stiffened TPB specimens", Acta Mechanica Solida Sinica, the official journal of the Chinese Society of Theoretical and Applied Mechanics, Vol. 8, Special issue, pp. 99-102.
[23] Abdel-Hamid I. Mourad, 2005, "Effect of stress state on mode II stable crack extension", Key Engineering Materials, Trans Tech Publication Inc, Vols. 297-300, pp. 1604-1610, online since November 2005.
[24] A.-H. I. Mourad, M. G. Alghafri, O. A. Abu Zeid, 2004 "Stable crack extension through AISI 4340 steel: Experimental investigation", Advances in Fracture and Failure Prevention, Key Engineering Materials, Trans Tech Publication Inc, IOS press, Kikuo Kishimoto, Masanori Kikuchi, Tetsuo Shoji and Masumi Saka, Vol. 261-263, pp 207-212, online since April 2004.
[25] Folias, E. S. , 1969, "On the Effect of Initial Curvature on Cracked Flat Sheets", International Journal of Fracture Mechanics, Vol.5, No.4, pp. 327-346.
[26] Erdogan, F. and Kibler, J. J. , 1969, "Cylindrical and Spherical Shells with Cracks", International Journal of Fracture Mechanics, Vol.5, No.3, pp. 229-237.
[27] Folias, E. S. , 1970, "On the Theory of Fracture of Curved Sheets" , Engineering Fracture Mechanics, Vol.2, No.2, pp. 151-164.
[28] Erdogan, F.; Delale, F. & Owczarek, J. A. , 1977, "Crack Propagation and Arrest in Pressurized Containers", Journal of Pressure Vessel Technology, Vol.99, February 1977, pp. 90-99.
[29] Shah, R. C. & Kobayashi, A. S. , 1973, "Stress Intensity Factors for an Elliptical Crack Approaching the Surface of a Semi – Infinite Solid", International Journal of Fracture, Vol. 9, 1973, pp. 133-146.
[30] Scott, P. M. & Thorpe, T. W. , 1981, "A Critical Review of Crack Tip Stress Intensity Factors for Semi – Elliptical Cracks", Fatigue of Engineering Materials and Structures, Vol.4, No.4, 1981, pp. 291 – 309.
[31] Newman, J. C. , 1973, "Fracture Analysis of Surface and Through-Cracked Sheets and Plates", Engineering Fracture Mechanics, Vol.5, No.3, pp. 667-689.
[32] RCC – MR , 1985, "Design and Construction Rules for Mechanical Components of FBR Nuclear Island", First Edition (AFCEN–3-5 Av. De Fried eland Paris 8), 1985.
[33] Milne, I.; Ainsworth, R. A.; Dowling, A. R. & Stewart, A. T. , 1986, "Assessment of the Integrity of Structures Containing Defects", CEGB Report No. R/H/R6 – Rev.3, Central Electricity Generating Board, London, U.K., 1986.
[34] Gajdoš, Ľ. & Srnec, M., 1994, "An Approximate Method for J Integral Determination", Acta Technica CSAV, Vol.39, No.2, pp. 151-171.
[35] Gajdoš Ľubomír et al., 2004, "Structural Integrity of Pressure Pipelines", Transgas, 80-86616-03-7, Prague, Czech Republic.